ÉCOLE POLYTECHNIQUE
FÉDÉRALE DE LAUSANNE

Faculté des Sciences de Base

Laboratoire de physique des Réacteurs et de comportement des Systèmes

Neutronic Analysis of the European Gas-Cooled Fast Reactor Demonstrator ALLEGRO and its Validation via Monte Carlo TRIPOLI Calculations

Master Thesis

KLAUSER Christine
September 2009 to February 2010

Professor: Prof. CHAWLA Rakesh
Supervision: BRUN-MAGAUD Valérie,
Dr. GIRARDIN Gaëtan, Dr. MIKITYUK Konstantin

Neutronic Analysis of the European Gas-Cooled Fast Reactor Demonstrator ALLEGRO and its Validation via Monte Carlo TRIPOLI Calculations

Contents

List of Figures

List of Tables

1 Introduction

Generation IV presents a new kind of nuclear power plants. It aims to considerably reduce nuclear waste while safety will be at least as high as at the current plants. The interest of such a plant brought together twelve countries, namely Argentina, Brazil, Canada, France, Japan, the Republic of Korea, the Republic of South Africa, the United Kingdom, the United States of America, Switzerland, the Peoples Republic of China and the Russian Federation and EURATOM. Together they form the Gen IV Forum, developing this new generation which should be operable around the 2050s.

The goals of Gen IV require two features: *Recycling* and a *fast neutron spectrum*:

- Recycling gives the possiblity to retrieve still burnable materials after a burning cycle which can be burned in a further cycle. In particular, one can get access to long-living actinides. For reasons of cost and safety, recycling in Gen IV plants ideally takes place on the plant's site. The recycled materials are treated all in one without separation of plutonium, therefore avoiding proliferation of dangereous substances.

- The fast neutron spectrum is needed for breeding and burning: The already mentioned long-living actinides can be burned with this fast neutron spectrum. This will make the burned fuel less radiotoxic on a long term basis. Further, the fast spectrum allows breeding of fissile material like ^{239}Pu from fertile material such as ^{238}U which constitutes most of the available uranium nowadays. Therefore, the efficiency of the fuel can largely be increased and the use of Nature's ressources reduced.

Generation IV reactors mostly operate at high and very high temperature for better thermal efficiency. Therefore, they can, apart from electricity production, play an important role in the desalination of sea water or hydrogen production.

There have been several proposals for Gen IV reactors: Lead Fast Reactor (LFR), Molten salt Thermal Reactor (MTR), Sodium Fast Reactor (SFR), Super Critical Water Cooled Reactor (SCWR), Gas Fast Reactor (GFR) and Very High Temperature Reactor (VHTR). Among these, the GFR is the main backup candidate with SFR being the more developed concept at the

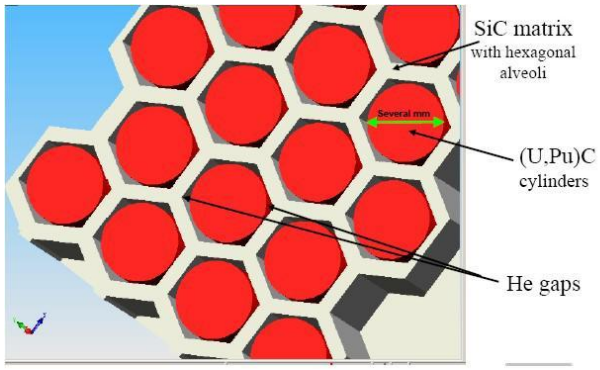

Figure 1: The advanced GFR fuel concept: Cylindrical (U, Pu)C pellets in honeycomb SiC structure

moment, taking advantages of the already operated sodium cooled systems like SUPERPHENIX or BN-600.GFR is a reactor disposing of a fast-neutron spectrum cooled by helium at high temperature for better thermal efficiency. This gas is advantageous in terms of nuclear and chemical interactions: It does not significantly soften the neutron spectrum and the corrosion of the structural material is negligible. In addition, in case of gas release, it does not present danger to the environment. Furthermore, the void effect[1] is minor for this coolant. The optical transparency of helium allows visual inspection and control of reactor components. However, its gaseous characteristics make it less efficient in terms of heat transfer compared to coolants in liquid states like lead or sodium. Also, the loss of coolant is a very dangerous accident for this kind of reactors because of the difficulty to remove decay heat from the core at acceptable temperature.

The fast neutron spectrum and the resulting high temperature are challenging for both structural and fuel materials. For GFR, there has been developed a new fuel concept on the basis of ceramics, called CERCER for CERamic-CERamic. Small pellets of a fissile ceramic material, viz. a mixed uranium-plutonium carbide fuel (U,Pu)C, are embedded in a ceramic matrix, made of SiC. As can be seen from Fig.1, fuel pellets are placed into hexagones of the matrix. This honeycomb structure is hermetically closed from both sides with a SiC cover to build a fuel plate as in Fig 2. Plates of this hexagons (see Fig.2) are assembled vertically composing the hexagonal

[1]The *void effect* denotes the change in reactivity of a reactor at operating conditions compared to to a situation where void is present in the reactor at the place of coolant.

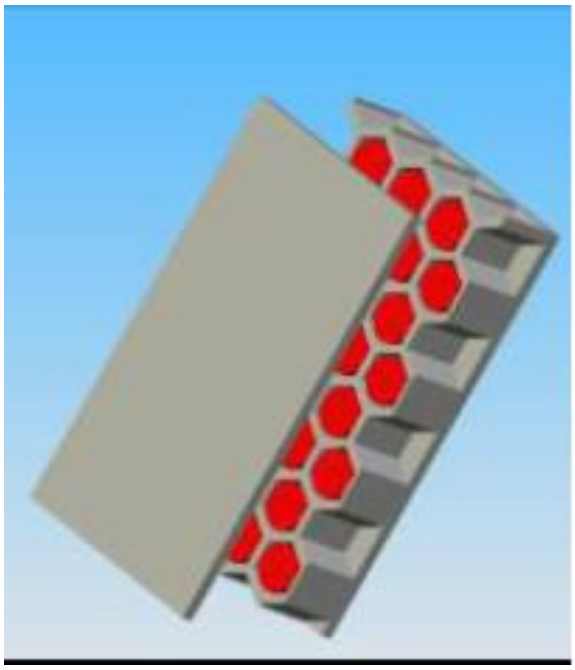

Figure 2: The advanced GFR fuel concept: Fuel plate

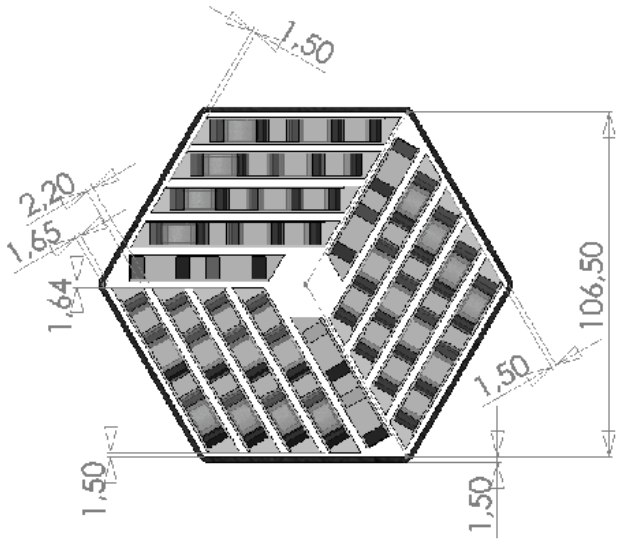

Figure 3: The advanced GFR fuel concept: horizontal cut of a GFR S/A with fuel plates

GFR subassembly (see Fig.3). The cooling is achieved via helium that is flowing in parallel to the plates on both sides. Another type of fuel, consisting of CERCER pins, is also under consideration [1].
The main goal of the thesis is to benchmark the algorithm for GFR fuel neutronic simulation recently implemented in the deterministic ERANOS system code against the Monte-Carlo continuous-energy solution by TRIPOLI and to make some analysis of the discrepancies observed. The ALLEGRO core (GFR demonstrator) was used in the analysis.
The structure of the thesis is as follows: The ALLEGRO demonstrator core is presented in Chapter 2. A general overview of the computer codes used is given in Chapter 3: on the probabilistic code TRIPOLI and the deterministic ERANOS code. Special features in ERANOS used for the modelling are described. Chapter 4 is a first comparison between the core reactivity calculated by the two codes. The heterogenous ALLEGRO model in both codes is described with special emphasis on the plate option in ERANOS. Heterogeneity impact is discussed for ALLEGRO. The analysis of the ERANOS-TRIPOLI discrepancy gets enhanced in Chapter 5, where investigations on simplified models are carried out that allow to learn more about the physics of the reactor. These simplified models are used to validate modifications in the ERANOS modelling taking place on an energetic as well a spatial level and the impact of these modifications on full Hex-Z models is looked at in Chapter 6. Of interest is in particular the modelling of the reflector in ERANOS. A modelling in 39 energy groups with adjusted energy boundaries is presented and impacts on initial parameters in the ECCO calculations are reported. Further, special attention is given to the control assemblies worth in the light of the modifications established. Finally, Chapter 7 provides the main conclusions to be drawn from this research, as well as the recommandations for future work.

2 Gas Fast Reactor ALLEGRO

ALLEGRO will be the first Gen IV gas cooled fast reactor ever built. The design phase is scheduled to finish in 2013 and the reactor should be built around 2020.It is designed to be a small sized prototype of about 80MWth. It will not be linked to any electrical cycle since this part of a nuclear plant is well known. The primary gas cycle will be cooled by a secondary water cycle. Part of the safety systems, the Decay Heat Removal (DHR) is in function in case of trouble with the gaseous coolant in emergency situations, ie Loss of Coolant Accident (LOCA). ALLEGRO shall not only give concrete demonstration of the feasability of a commercial GFR but also be there to learn about the fundamental physics of such GFR. Namely, it shall give experimental data of the newly developed structural and fuel materials and qualify numerical methods used for its design and simulation. ALLEGRO will successively contain two cores: A start-up and a demonstrator core, establishing and qualifying on a step by step basis the new GFR technology starting from familiar concepts:

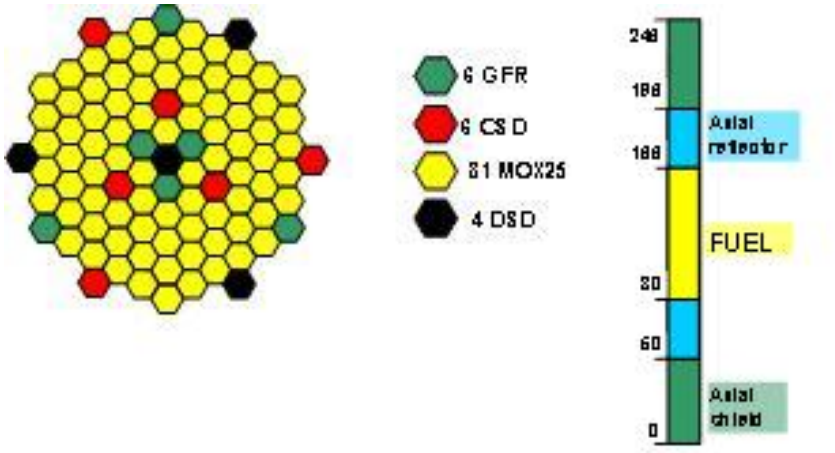

Figure 4: The ALLEGRO Start-up-core with positions of GFR fuel test S/As, Control System Device (CSD) and Diverse System Device (DSD)

- *The Start-up core* (see Fig.4) contains mostly common Mixed uranium-plutonium OXide fuel (MOX) with 24 vol% of plutonium in pin shape.

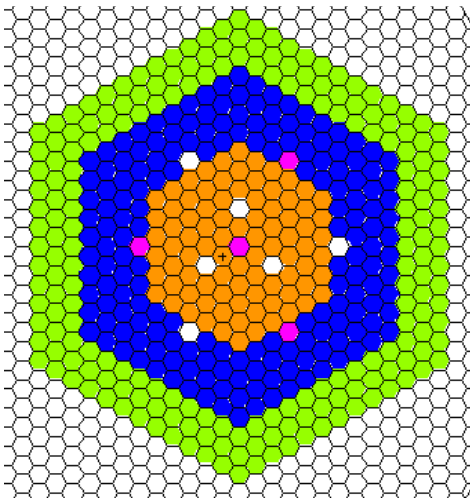

Figure 5: Demonstrator core of ALLEGRO. The GFR fuel S/A s are in orange, the CSD and DSD S/As are white and pink respectively, the reflector is blue and the shielding green.

After 220 Effective Full Power Days (EFPD), six experimental GFR subassemblies (S/A) containing ceramic (U,Pu)C with 30 vol% of Pu inserted at positions formerly occupied by stainless-steel will be S/As inserted to reduce a high core reactivity at the beginning of life. Three of them are located close to the core center, experiencing therefore a high neutron flux with a flat gradient and the other three are placed in the core pheriphery, thus exposed to a low neutron flux of a steep gradient. These experimental S/As will stay in place while the MOX S/As will get replaced by fresh ones after a total of 660 EFPDs and once again after 1320 EFPDs. Thus, the GFR S/A should be evaluated over these 3 MOX cycles or about $3 * 660 - 220 = 1760$ EFPDs.

- *The Demonstrator core* (Fig.5) is completely composed of GFR S/As, with 10 control S/As positioned identically as in the start-up core. It is the model used for this present work. The seven rings of fuel are surrounded by four rings of ceramic reflector. The reflector consists mainly of a ceramic compound of natural zirconium ZrC. Structural components of SiC and helium are also present. The proportion of these three ingredients are different for the radial and axial reflector with 65% (17.5, 17.5) and 45 % (38, 17) ZrC (He, SiC) respectively.

The reflector rings are followed by 3 rings of shielding (B_4C). Operating with a mean temperature of 1263 K, it has a thermal power of 75 MW [2].

3 Computational Tools

This thesis work has been done using the deterministic European Reactor Analysiss Optimized code System ERANOS in the version 2.1 as well as the probabilistic code TRIPOLI-4. Both codes are used in association with a consistent neutron nuclear data library in order to solve the Boltzmann transport equation. In the case of ERANOS, individual codes and calculational procedures are used to obtain the core's neutronic parameters, e.g. the effective multiplication factor k_{eff} or the fine flux at each point of the system. These parameters can be reached in TRIPOLI by defining specific tallies.

3.1 TRIPOLI

TRIPOLI is a Monte Carlo code, it can be used for simulations involving neutrons, photons, electrons and positrons. The version used is TRIPOLI-4. In contrast to deterministic codes, probabilistic ones like TRIPOLI do not solve the transport equation explicitly. They rather generate particles (neutrons in this case) one by one and follow their walk through the reactor core and interact with the atoms of a given medium in order to simulate different kinds of interaction such as scattering, absorption or fission based on a random number generator. The total of the histories reveals the reactor's behaviour. For a big number of particle histories, the simulation of a probabilistic code converges to the actual solution by the central limit theorem. The use of Monte Carlo (MC) based codes implies therefore a careful treatment of convergence indicators. Eventhough more expensive in time on simple geometries, MC codes are very useful for complicated systems where a deterministic, explicit solution is impossible. Furthermore, they constitute an excellent benchmarking tool.
TRIPOLI makes available either continuous cross sections or cross sections by energy groups. For the present work, continuous cross sections were chosen from JEFF-3.1. Sources can be defined by a multiplication of radial, angular, energetic and time factors. Geometries can be defined either by vol-

umes or surfaces or a combination of the two. Multiple operators like union, intersection, erasement and subtraction permit various combinations to build the geometry. The accuracy of the TRIPOLI simulation is optimised by the use of a variance reducing biasing scheme based on an importance function which relies each point in phase-space with a weight. The importance function involving spatial, energetic and time factors can be directly calculated by the code. Computations carried out for the present work do have typically an accuracy of $\sigma = 40$ pcm. During simulations, each particle is provided with a simulation weight. The sampling is done in a way to let the ratio of the importance function weight and the simulation weight be as close to 1 as possible. This goal can be reached by techniques of russian roulette and splitting on the situations *just before transport* and *just before collision*. TRIPOLI enables the use of a multitude of tallies which can be specified. The physical quantities which can be calculated are e.g. neutron flux, multiplication factor k_{eff}, current, reaction rate, dose equivalent rate, deposit of energy and recoil energy etc. The present work used essentially k_{eff} and the tallies for neutron flux. Further, TRIPOLI features perturbation calculations, parallel CPU simulations, conditional scores and resuming a stopped run [3], [4].

3.2 ERANOS

ERANOS is a deterministic system code developed for fast neutron spectrum cell and core calculation which was recently enhanced for the specific requirements of Gen IV systems like the plate geometry [5],[6]. Different nuclear data libraries, namely the evaluated neutron libraries JEFF-3.1, JENDL-3.3 and ENDF/B-6.8, have been included in the ERANOS package in adddition to calculational procedures and codes like BISTRO [7] or TGV/VARIANT [8]. As of lack of data specific for Gen IV research reactors, a nuclear data library based on JEFF-3.1 is used and treated with NJOY and CALENDF and include experimental data mainly from Superphenix measurements and other liquid metal cooled reactors [5]. Different libraries are available in different energy structures (groups): 1968-group for the main resonant nuclides (e.g. ^{235}U, ^{238}U, ^{56}Fe, 33-groups library, that used in reference calculations, and serves for fast spectrum applications, as well as a 175 energy group library called VITAMIN-J scheme and a 172 energy group library called XMAS scheme, appropriate for shielding calculations and thermal-spectrum applications respectively. The deterministic code ERANOS solves the trans-

port equation for the reactor core explicitly in a two step approach: a) the cell/lattice calculation performed with the ECCO code [9] and b) the core calculation, using either the variational nodal method TGV/VARIANT for a 3D core geometry or the finite differerence Sn BISTRO method for a 2D core geometry.

ECCO calculates the macroscopic multigroup selfshielded cross section for cells specified by the user. These cells correspond to physically similar zones, e.g. S/As like fuel, CSD and DSD. The geometric details of the cell can be defined homogeneously or heterogeneously. Heterogeneous cell descriptions are possible for a variety of geometries by the use of 2D units like cylinders, rectangles or slabs; common pin-shaped fuel can easily be modelled. The ERANOS version used for the present work, 2.1, provides also a tool to model the innovative plate-shaped GFR fuel. A third of the hexagonal fuel S/A gets projected into a rectangular frame. A detailed description of the use of this tool is given in Chapter 4.1. The filling media of the cell are mixtures of materials. ECCO calculates the corresponding macroscopic cross-section of one cell by taking the microscopic ones of each isotope from the provided library. Concretely, this happens on a step-by-step sequence. For most of the calculations of the present work, the design route of ECCO has been chosen[2]:

- First, the fission source is calculated and then the axial buckling value B^2 is searched to have a cell in the fundamental mode. ECCO considers the cell in an ideal 2D infinite medium and ajdusts the axial buckling to get a critical cell. This step is carried out in 33 energy groups on the nuclear data from the JEFF-3.1-library.

- Secondly, the calculation is refined by taking 1968 energy groups into account with the found buckling. The self-shielding is calculated with the subgroup method [10]. At the end of this step, the cross sections calculated get condensed from the fine energy group structure into an energy structure of a lower number of groups. The reference is a condensation to 33 groups, but the user is free to choose another number.

- Over these new cross-sections, the critical buckling is searched once more in a third step in the energy structure condensed to in the previous

[2]Except for the fourth step, the geometry of the cell can be both homogeneous or heterogenous. The keyword HOMOGENISE in the last step creates a homogeneous step regardless the original geometry of the cell. In the present work, it was chosen to always use the original geometry in the first three steps.

step.

- Finally, the fourth step homogenises the complete cell, establishing in this way one macroscopic cross-section set for the cell. It is possible in a fifth step to condense the cross section to one energy group for verification purposes mainly.

Two different routes were used in the present calculation based on the degree of details assumed. Homogeneous cells have been treated by only using the first two steps. The design route was the route chosen for heterogeneous cell calculations. As for non-fissile cells, the flux of a neighbouring fissile cell is taken and the axial buckling adjusted correspondingly. Self-shielding treatment is established by a fine energy group consideration of the slowing-down taking into account 1968 energy groups in combination with a subgroup method that assumes a uniform neutron source and uses probability tables in order to account for the resonant structure of heavy nuclides. The self-shielded multigroup cross sections issue of this calculation are condensed and blurred to obtain the macroscopic cross sections.
In a second phase, the S/A represented by the different cells are put together into a three-dimensional geometry (for instance, Hex-Z in the example of ALLEGRO) and the transport equation under the corresponding conditions is solved. For this latter part, ERANOS offers two possibilities: (1) BISTRO or (2) VARIANT. BISTRO uses a finite difference Sn approach to solve the transport equation [7], whereas VARIANT has a nodal approach, looking for a solution composed of an expansion of precalculated angular and spatial basis functions [5]. For the present work, VARIANT has been chosen for full Hex-Z core models. The solution of the transport equation commonly is done choosing the option WITH_SIMPLIFIED_SPHERICAL_HARMONICS. This choice allows in many cases still very good results but with much less cost in time. RZ-calculations were carried out using BISTRO [5], [10].

4 ALLEGRO Models and Benchmarking

This chapter aims to compare the calculational neutronic results obtained with TRIPOLI and ERANOS on the ALLEGRO demonstrator core. The indicator chosen is the core's effective multiplication factor k_{eff}. Benchmarking of ERANOS vs. probabilistic codes have already been carried out for the large size reactor GFR of 2400 MWth. Discrepancies remain in acceptable range [11], [12]. As for ALLEGRO, first benchmarking was undertaken on the demonstrator core in a previous study. Specifically, an ERANOS Hex-Z model was developed containing homogeneous fuel S/As while the control assemblies were treated both homogeneously and heterogeneously [13]. These ERANOS models were benchmarked against corresponding TRIPOLI models. The discrepancies of the two codes show the same behaviour and amplitude as for the GFR-2400 core [12]. Further, a heterogeneous TRIPOLI model was used for comparison. Heterogeneity denotes in this context as well in all following referencies to a heterogeneous ALLEGRO model that not only the control assemblies but also the fuel S/As were treated as heterogeneous. In concrete: They are modelled as can be seen in Fig.3: Three times five fuel plates between which helium circulates, arranged in a rotational symmetry in a SiC wrapper. However, the fuel plates themselves are simulated by a homogenous mixture of (U,Pu)C, SiC structural material and helium. The second step of heterogeneity modelling, i. e. the exact representation of the SiC honeycomb structure containing fuel pellets as shown in Fig.2 is not carried out. Between the homogeneous and heterogeneous TRIPOLI models a heterogeneity effect of about 40 pcm was found [14].

For the present work, a heterogeneous ERANOS Hex-Z core model was developed as well as RZ-models of ALLEGRO for both codes in order to better understand the discrepancy. Calculations were carried out for isothermal cores of 300 K at beginning of life.

4.1 Heterogeneous Cell Calculation in ERANOS

The ECCO code of ERANOS provides tools for modelling for both, homogeneous and heterogeneous fuel cells. This allows a very exact modelling of common pin-shaped fuel. The latest ERANOS version 2.1 contains also an option for plate-type fuels. The heterogeneous modelling of plates in ECCO proceeds as follows (see Fig.7): A third of the hexagonal S/A (of rhombic shape, a simplified scheme can be found in Fig.6) is approximated by a

rectangular frame (see Fig.7). There is one top and one bottom stripe of varying thickness $h1$ and $h2$ considered. Inbetween them, there are placed as many vertical stripes as needed of various thicknesses e but all with the same height h. Let's now have a look at the GFR plate S/A as it is planned to be constructed: Fig.3 indicates a SiC tube containing twelve long and three short plates of SiC fuel as well as an inner SiC hexagonal tube to provide mechanical stability. The spaces between structural material and fuel plates are filled with He. In the procedure of the modelling, a certain number of

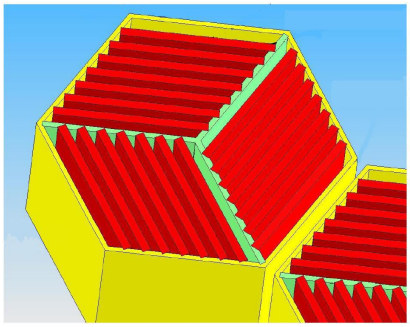

Figure 6: The plate-type S/A as it is modelled in ERANOS. Yellow: Wrapper. Red: Homogeneous fuel plate. Green and transparent parts: He

assumptions and simplifications have to be done. All these changes were carried out under the strict conservation of the volumic ratios of the different materials. The changes undertaken were the following ones (The model for ERANOS is partly illustrated in Fig.6.):

- The *inner SiC structure*, namely the inner vertical tube were neglected in accordance with previous work [14]. The volumes are considered to be filled by helium. The volumic ratios correspond to the description in [14]. For all the further rearrangments listed, the integral masses are preserved.

- As there is only one *width* allowed, it is determined by averaging the fuel plates' widths. However, their thickness did not get changed, thus an exact as possible simulation of the neutrons' path in a plate is possible. The conservation of mass throughout rearrangement imply a change in the helium stripe thicknesses (*e1, e2, e3*). Another possible choice is

to let the thicknesses of the gas inbetween the fuel plates at their originial value and to adjust thickness (d) and width (h) of the fuel plates accordingly. This choice might alter the neutrons' path in the fuel plate and give different self-shielding properties than the first choice. However, the neutrons' behaviour in the gas stripes would be more accurately calculated especially in terms of streaming. As both ways of modelling present advantages and disadvantages, they were both taken into account while performing calculations on heterogeneous Hex-Z core models.

- The *remaining helium*, namely the one located just above the horizontal wrapper and the one above the short fuel plate was redistributed among the horizontal stripes weighted by their original thicknesses. It has to be reminded that this may change the neutrons path inbetween the fuel plates. However, He being nearly completely transparent to neutrons, the impact is expected to be minor.

- For the sake of consistency, the wrapper and helium present between the S/As were merged into a single medium called 'TH-LAME'. It constitutes the border vertical as well as the bottom stripe, where the thickness $h2$ of the latter corresponds to the thickness $h2$ of the first. This merger is necessary as it is not possible to have several horizontal stripes in the modelling.

The heterogeneity effect for the ALLEGRO fuel cell is small: 33 pcm difference were calculated for k_{inf}. Indeed, the neutron flux in the different regions of the heterogeneous fuel cell is nearly identical with the one in the homogeneous fuel cell. In Fig.8 the discrepancy in flux normalized to the homogeneous value is shown for a helium region and a fuel plate region. The discrepancies remain low in general. Heterogeneity effect is visible for the resonances of fissile and fertile material observable as peaks and valleys at the corresponding resonant energies.

For closer analysis of the heterogeneity effect, a sensitivity study in ERANOS was performed comparing homogeneous and heterogeneous fuel modelling. Exact perturbation theory was used on an infinite fuel cell and the results are reported in Fig.9. Analysis show that for the inifinite fuel cell, especially ^{238}U and ^{239}Pu contribute to changes in reactivity. In the heterogeneous fuel cell, the (U,Pu)C components are locally more concentrated than in the homogeneous model which translates to a higher selfshielding

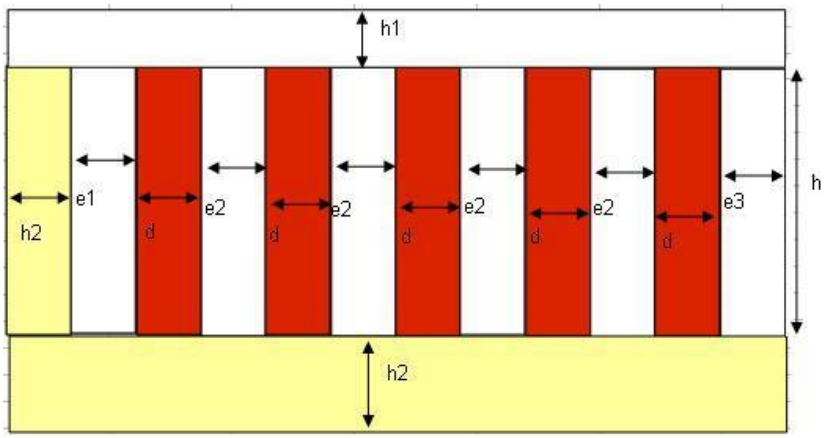

Figure 7: The modelling of a third of a plate-type fuel S/A in ERANOS. yellow: wrapper+helium, white: helium, red: fuel plate

provoking a decrease of reactivity. However, the study permits to exclude significant compensatory effect.

In comparison to the large size core GFR-2400, the heterogeneity effect in ALLEGRO is considerably smaller. The small size of ALLEGRO requires a high amount of Pu (25.9 vol% in the model used) that contrasts with 15 vol% of Pu for a typical GFR fuel S/A. This important difference in Pu content alters the neutron spectrum (see Fig.10). The percentage of neutrons with an energy higher than 0.1 MeV in GFR-2400 is 50 % comparing to 56.6 % in ALLEGRO. The harder ALLEGRO spectrum thus reduces heterogeneity effect compared to the GFR core characterised by softer spectrum.

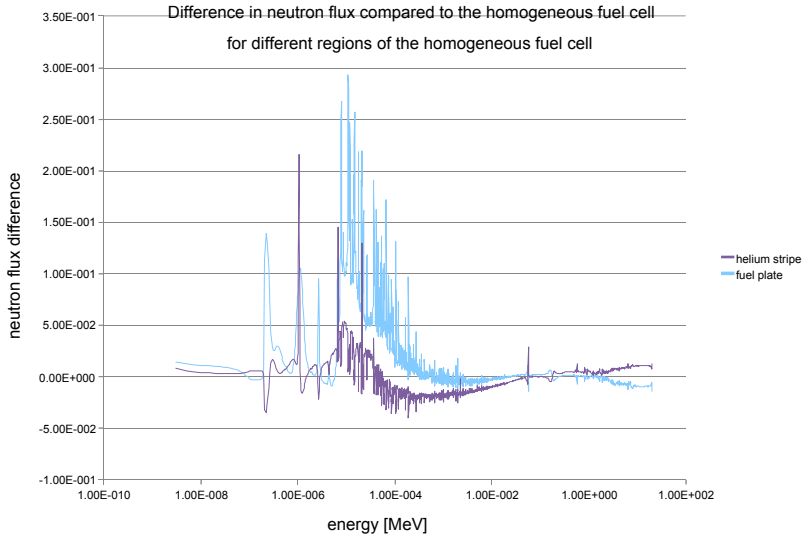

Figure 8: The difference of the neutron flux in different regions of the heterogeneous fuel cell to the homogeneous fuel cell normalised to the homogeneous value. For most regions, the plot is congruent with the one of the fuel plate which was chosen to be plotted here, except for the wrapper regions.

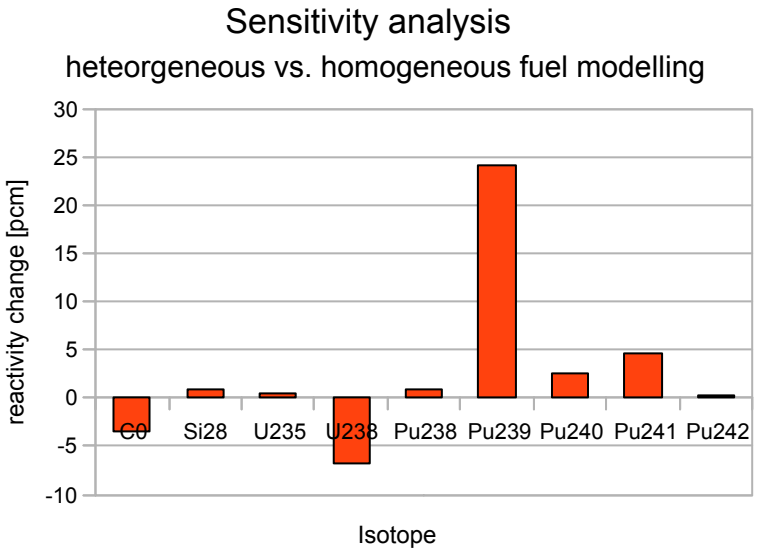

Figure 9: Sensitivity analysis hom-het for an infinite fuel cell

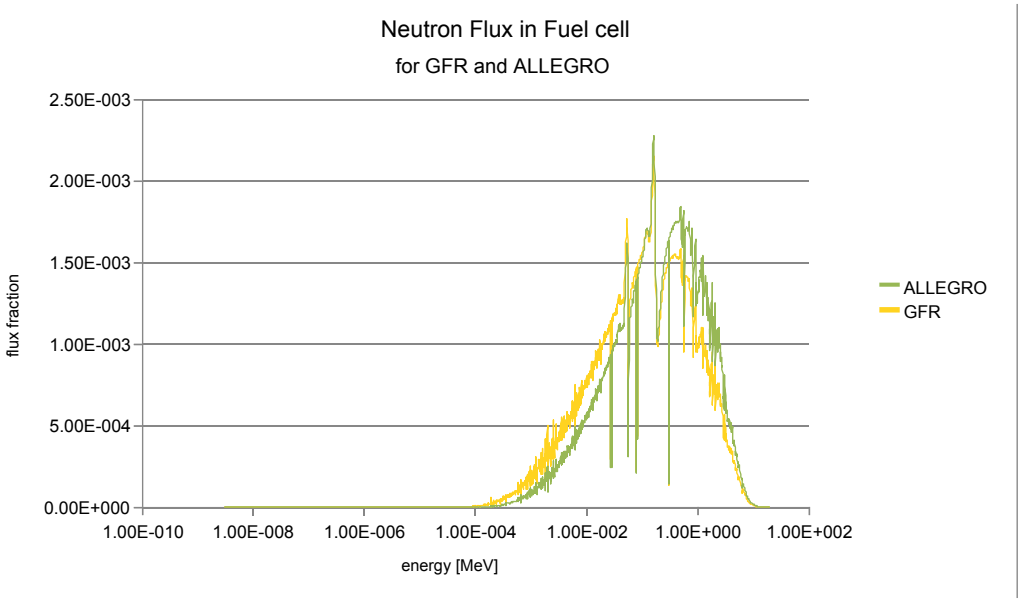

Figure 10: The neutron flux fraction per energy group by fine group calculation for both the ALLEGRO and GFR homogeneous fuel cell

4.2 Comparison of ERANOS-TRIPOLI Core Calculation

The model developed in the previous section is compared to corresponding TRIPOLI values available from [14]. The reactivity effects calculated are reported in Table 1 for the Hex-Z model of ALLEGRO with two configurations of the control assemblies: Either all of them inserted in the core or all of them in parking position, i.e. withdrawn from the fuel. As the models are all isothermal, the change in reactivity from the homogeneous Hex-Z to the heterogeneous Hex-Z is purely due to geometric effects. A loss of reactivity is expected due to the transition to a heterogeneous model. The loss of reactivity in the calculations from both codes is minor, a maximal value of -102 pcm for the ERANOS calculation with the control assemblies inserted is manifest.
The discrepancy ERANOS-TRIPOLI carried out on the same configurations of the control assemblies shown in Table 2 remain thus in the same range as calculations on homogeneous Hex-Z models. Further, Table 2 provides values for both cases discussed in the previous section: original plate thickness and original helium thickness. The results remain in the same order of magnitude. The plate option in ERANOS is thus stable under these modelling possiblities. The heterogeneity effect in ERANOS being of the same range as in TRIPOLI validates therefore the ERANOS option for GFR plate fuel for ALLEGRO.

Table 1: Change of reactivity due to the transition from the homogeneous Hex-Z to the heterogeneous Hex-Z model for both codes.

Code	$\Delta\rho$ [pcm]	$\Delta\rho$ [pcm]
	(CSD+DSD) out	(CSD+DSD) in
TRIPOLI	-42	-25
ERANOS	-4	-102

ALLEGRO is a small sized reactor and thus the curvature of the flux is important (see Fig.11). Previous calculations [14] have been done using simplified options for the solution of the transport equation in VARIANT with an order of polynominal expansion for the even flux of 6, for the partial current of 0 and for the nodal source of 1. Spatial approximation using the VARIANT option for transport WITH_SIMPLIFIED_SPHERICAL_HARMONICS can lead to non-negligible discrepancies. Therefore, the same calculation on the

Table 2: Reactivity discrepancy (ERANOS-TRIPOLI) for the two considered modelling options in ERANOS compared to the TRIPOLI model : fuel plate width constant or He strip width constant

configuration	fuel width cst		He width cst	
	$\Delta\rho$ [pcm]	k_{eff} ERANOS	$\Delta\rho$ [pcm]	k_{eff} ERANOS
CSD +DSD OUT	-438	1.06686	-427	1.06699
(CSD+DSD) IN	-81	0.89225	+3	0.89292

homogeneous Hex-Z core were carried out in an exact solution of the transport equation (options of 612). The results are shown in Table 3 in comparison to the simplified option. The discrepancy is reduced for the configuration of all control assemblies (CAs) out. Further, the discrepancy is of the same order for both CA configurations in the case of exact transport whereas in the case of simplified transport, the discrepancy varies in function of CA configuration. Whether CAs are inserted or not translates to different core configurations to be calculated. Hence the use of exact transport overcomes geometric difficulties and allows to take into account high flux gradiants appearing at full insertion of CAs and therefore to better predict the CA worth. However, for reasons of calculation time, the following core analysis on Hex-Z cores were all calculated in the 601 option if not mentioned otherwise.

Table 3: Discrepancies ERANOS-TRIPOLI in the case of the option using simplified spherical harmonics (601) and using the exact transport option

Configuration	simplified	exact
	$\Delta\rho$ [pcm]	$\Delta\rho$ [pcm]
(CSD +DSD) OUT	-476	-308
(CSD+DSD) IN	-3	-323

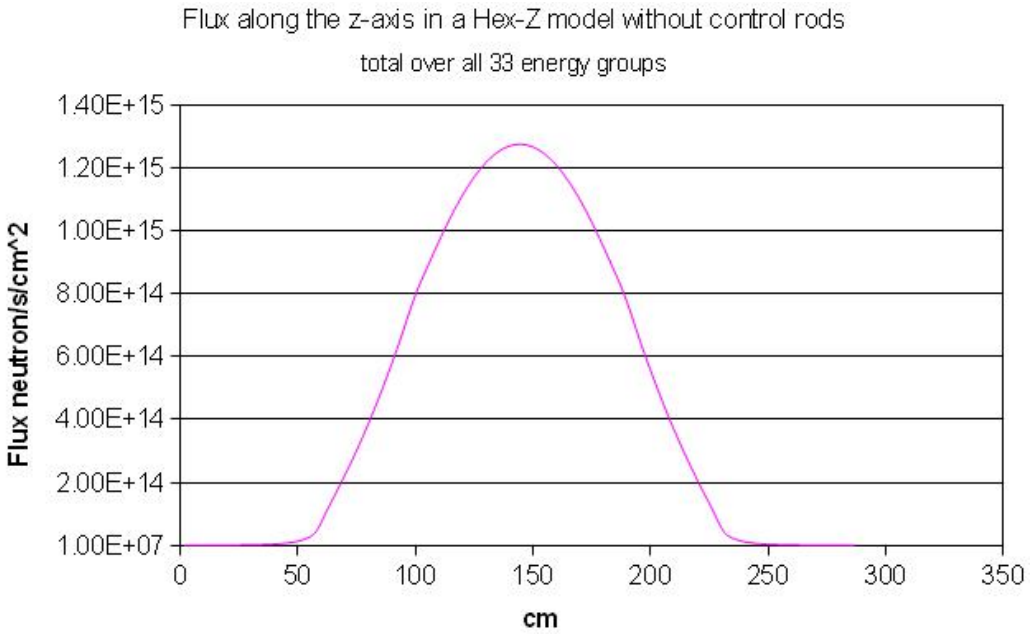

Figure 11: The flux for 75 MWth along the z-axis in a simplified homogeneous Hex-Z model where no control S/As are present, for the total height of central fuel S/A(289 cm)

5 Physics Analysis of the ERANOS-TRIPOLI Reactivity Discrepancy

In order to better explain and understand the discrepancies in reactivity of ERANOS and TRIPOLI (see Table 2), a step-by-step approach is established to get from the most simple geometry to more complicated structures. It starts with the basic infinite fuel cell and gets then modified.

5.1 Infinite Medium

An infinite (homogeneous) medium is created and its k_{eff} calculated (thus equivalent to k_{inf}). In order to generate such a medium, the boundary conditions on limiting surfaces are 'DERIVEE_NULLE' and 'REFLEXION' in ERANOS and TRIPOLI respectively. For the ERANOS/ECCO calculation under the condition of infinite medium, an adequate choice of parameter for the infinite cell is to put the buckling to zero ($B^2 = 0$). The reactivity difference between ERANOS and TRIPOLI is of -12 pcm, thus a very good agreement between the two codes was found.

5.2 Cylindrical Reactor Models

After confirming consistency of the two codes on a basic set-up, several modifications on geometry and materials used are done in order to get closer to the actual ALLEGRO demonstrator core. First, an axially infinite cylinder of fuel was simulated surrounded by either (1) shielding material or (2) reflector, followed by a second step of successive infinite concentrical cylinders of fuel, reflector and shielding, as represented in Fig.12. This gives 3 axially infinite models. They are referred to as *infinite*. The radii chosen correspond to the equivalent surfaces of the media in ALLEGRO. The same scheme is applied on geometries which are finite in all directions and that thus have also axial reflectors and axial shielding. Rings of radial shielding and radial reflector (also axially finite) are added like in the previous infinite case. The heights chosen are equivalent to ALLEGRO. The 3 models axially finite models with axial shielding and axial reflector are referred to as *finite*. This makes a total of 6 different simplified cylindrical models. In this section, the influence of the refelctor and shielding is analysed.

The results are reported in Table 4. In the case of axially infinite cylinder,

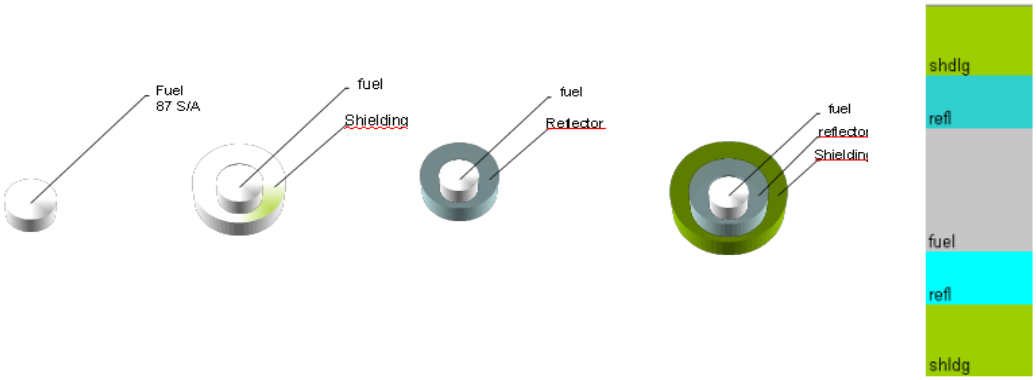

Figure 12: Simplified cylindrical models for analysis purposes.

we obtain an important effect coming from the reflector: For basically the same geometry, a fuel cylinder in addition to a further ring, the introduction of the reflector alters the discrepancy to the corresponding TRIPOLI model by 189 pcm compared to 27 pcm with a shielding ring. The very similar geometries suggest that this discrepancy cannot only be explained by geometrical factors. The ZrC reflector itself seems not to adequately be taken into account by ERANOS. The same effect of the reflector is stated for the finite geometries, but in a higher amplitude. For the model which comes closest to the actual ALLEGRO, i.e. three finite cylinders, the discrepancy is already in the order of magnitude observed for the homogeneous Hex-Z model.

A last step consisted in establishing a full RZ model of ALLEGRO. This is the cylindrical model of the ALLEGRO demonstrator core, the volumes are conserved with respect to the Hex-Z model. A vertical cut is shown in Fig.13. It contains homogenised fuel. The position of the control assembly rings were chosen as following: the DSD ring of the middle is put into a ring of the equivalent of six fuel S/As, followed by a thin ring of CSD equivalent. The remaining fuel constitutes the second fuel ring after which the outer CSD S/A equivalent is placed, followed by the corresponding DSD equivalent. The change from RZ to the homogeneous Hex-Z model increases the reactivity for both codes in the range of 25 pcm, the discrepancy between the codes remains thus constantly 500 pcm. A complete overview of different kinds of modelling is shown in Table 5. The relatively simple case of finite cylindrical rings of fuel, shielding and reflector is compared to full RZ and Hex-Z models

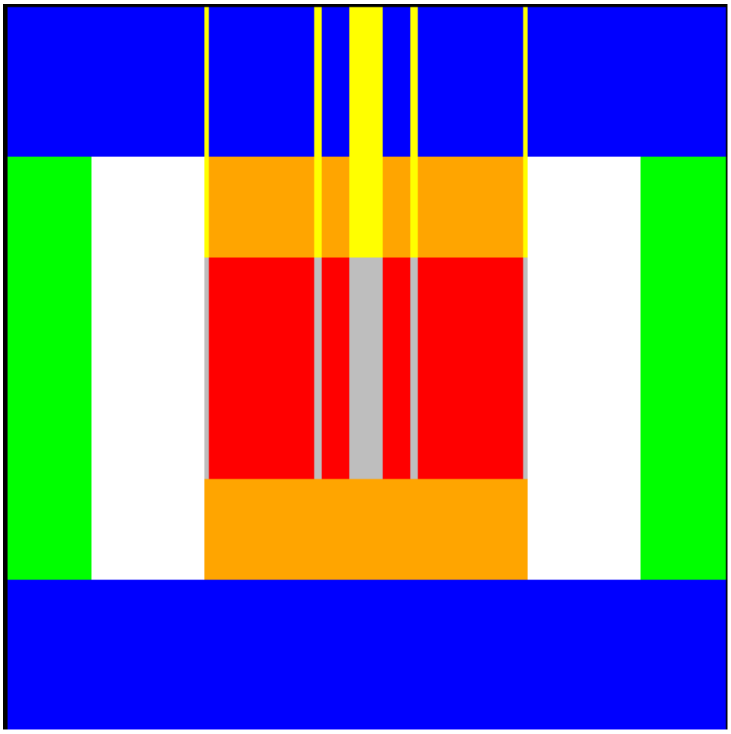

Figure 13: A full RZ model (vertical cut) of ALLEGRO in the configuration of all control assemblies in parking position. Red: Fuel. Yellow: control assemblies. Grey: Follower. Orange: Axial Reflector. White: Radial reflector. Blue: Axial Shielding. Green: Radial Shielding.

Table 4: Reactivity discrepancies between ERANOS and TRIPOLI for infinite and finite cylinders of fuel, surrounded by different combinations of reflector and shielding material

Model	$\Delta\rho$ [pcm]
z infinite	
shielding	-27
ZrC reflector	-189
ZrC reflector+shielding	-238
z finite	
shielding	-198
ZrC reflector	-507
shielding+ZrC reflector	-553

of ALLEGRO in terms of discrepancies in reactivity between the two codes. Clearly, the discrepancy remains in the order of 500 pcm, ERANOS values being systematically lower. Therefore, the discrepancy between the two codes

Table 5: Reactivity discrepancies between ERANOS and TRIPOLI for three modelling possibilities.

Model	$\Delta\rho$ [pcm]
simplified RZ shielding+refl+fuel	-553
complete RZ	-506
homogeneous Hex-Z	-476

observed can be attributed essentially to the reflector material, ZrC.

5.3 Reflector and Thermal Neutrons

An analysis of the flux for the simplified RZ-model in ERANOS (axially finite cylinders of homogeneous fuel, reflector and shielding) is reported in Fig.14 in terms of fraction per energy group. As it is expected for a fast reactor, the flux is mainly concentrated around fast energy groups. In contrast, the reflector states an important contribution of flux in the thermal group 31 which translates to an energy interval from 0.54 eV to 4 eV. This peak is

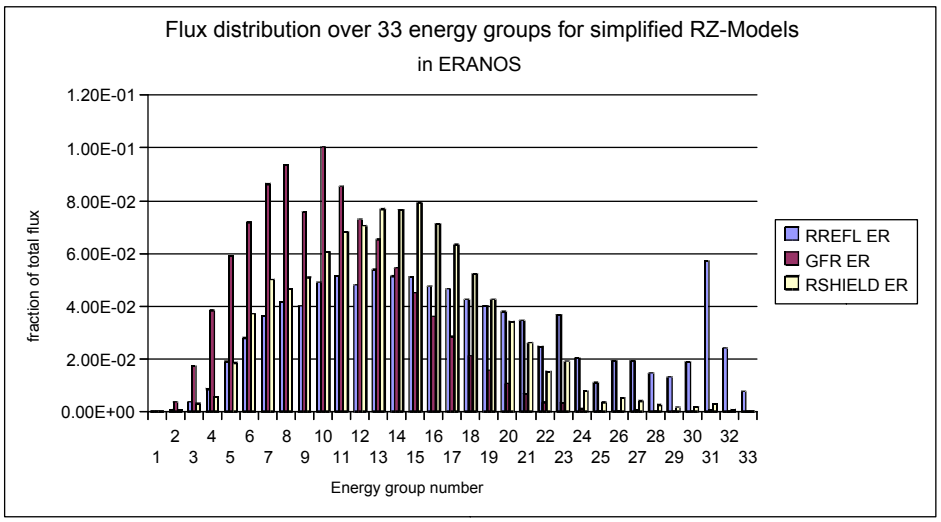

Figure 14: The neutron flux fraction per energy group in the simplified finite cylindrical model in ERANOS calculation

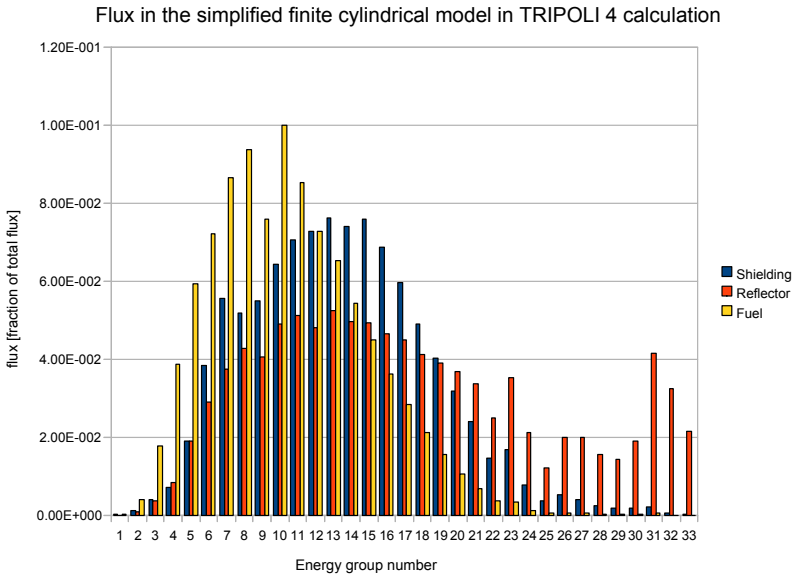

Figure 15: The neutron flux fraction per energy group in the simplified finite model in TRIPOLI calculation

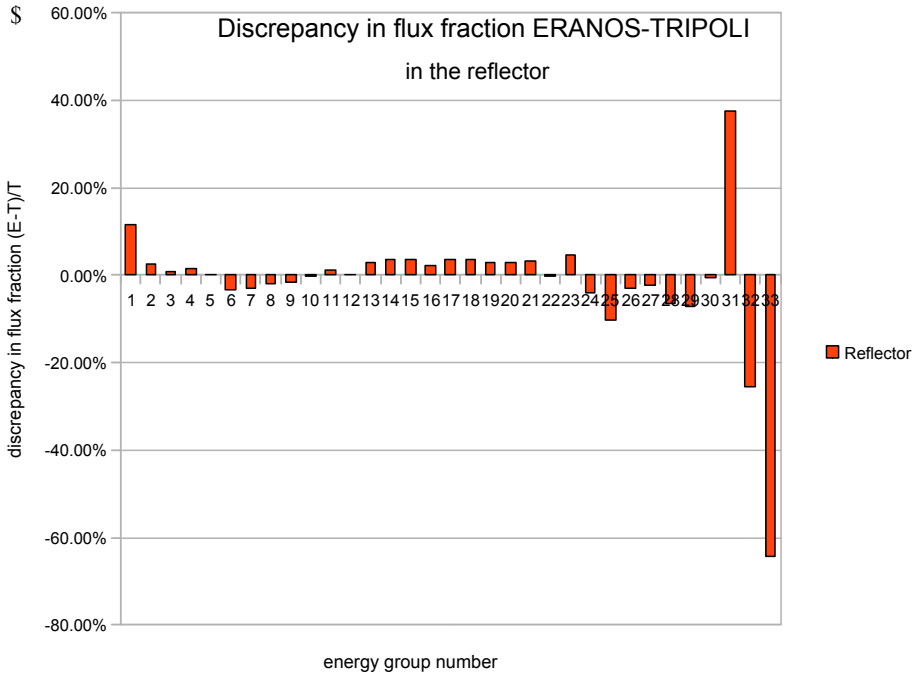

Figure 16: Difference in flux fraction per energy group ERANOS-TRIPOLI renormalized to the TRIPOLI value ($\frac{\Phi_{eranos}-\Phi_{trip}}{\Phi_{trip}}$)

confirmed by equivalent studies using TRIPOLI (see Fig.15). However, the comparison of the fluxes fraction per energy group between the two codes (see Fig.16) does show significant discrepancies for the thermal energy groups, confirming the fact that reactivity differences are due to the ZrC reflector. Sensitivity studies in ERANOS on both the infinite fuel cell and the complete RZ-ALLEGRO model show different behaviour (Fig.17, a complete overview of the contributions is given in Appendix A), eventhough they are sensitivity studies over the same condition: the use of heterogeneous or homogeneous fuel. Comparing sensitivity studies of the infinite fuel cell and the complete RZ core, the impact of the isotopes involved differs. To mention especially are the ^{238}U and the C which have a different sign of the reactivity change in the respective set-ups. A closer analysis of the cross section change for ^{238}U tracks down the major difference to be located in and around the 31 energy group. This difference in behaviour originates from the presence of ZrC reflecting material: A qualitative analysis consisting in a renormalisation

of the contributions using the respective flux from the infinite cell and the complete core calculation permits to conclude that the thermal neutrons scattered back from the reflector are responsible for this phenomenon.

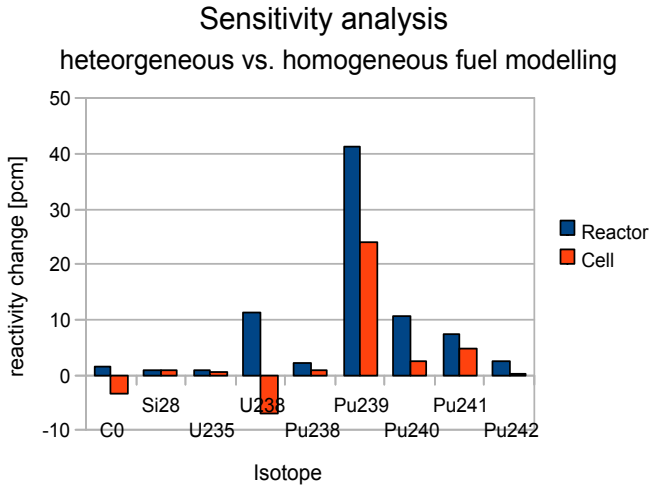

Figure 17: Sensitivity analysis by hom-het by ERANOS for a complete RZ-model of ALLEGRO in the configuration of all control assemblies out

6 Reflector Modelling

The previous chapter suggests that reactivity differences might come from the reflector's modelling. The adequate modelling of the reflector is a well-known issue of ECCO (e.g. [17], [16]). For the present work, two different approaches were taken: A change of the energy discretisation as well as a spatial approach introducing macrocell method. Both ways of modelling have already shown satisfactory results carried out on metallic reflectors for sodium reactors [16], [17].

6.1 Refinement of the Energy Structure

Zr presents multiple resonances. They are reported for the main component of the reflector, the isotope ^{91}Zr in Fig.18. The perpendicular lines plotted show the energy discretisation of 33 groups. The inexact treatment of these resonances being smeared into the group intervals may explain the discrepancy to the TRIPOLI code using continuous-energy cross sections. The most exact treamtment possible with ECCO would be a fine groupe structure calculation containing 1968 energy groups as being used as a reference in [16]. However, such an approach has been revealed impossible on the current problem due to the physical restriction of computer memory. A first test with 299 energy groups on simplified cylindrical models reported in Table 6 shows better agreement between the two codes compared to the previous values from Table 4 tested on cylindrical models with all three components (fuel, reflector and shielding) present. Nevertheless, calculations on more complicated structures such as Hex-Z core geometries were revealed impossible due to memory restriction. Therefore, the number of energy groups was only locally increased around the resonances of ^{91}Zr. The proposed technique uses 39 energy groups. The boundaries at 3.04 10^2 eV, 4.54 10^2 eV, 5.53 10^3 eV and 2.03 10^3 eV were taken off as they lay on resonances of Zr. Instead, nine supplementary boundaries were introduced. They are shown in Table 7. These permit to better take into account the resonances' effect, by centering one and only one resonance in the energy group interval. As for the quasi-continuous resonance region, an exact treatment of resonances is not possible. Therefore, the existing discretisation coming from the 33 groups is used.

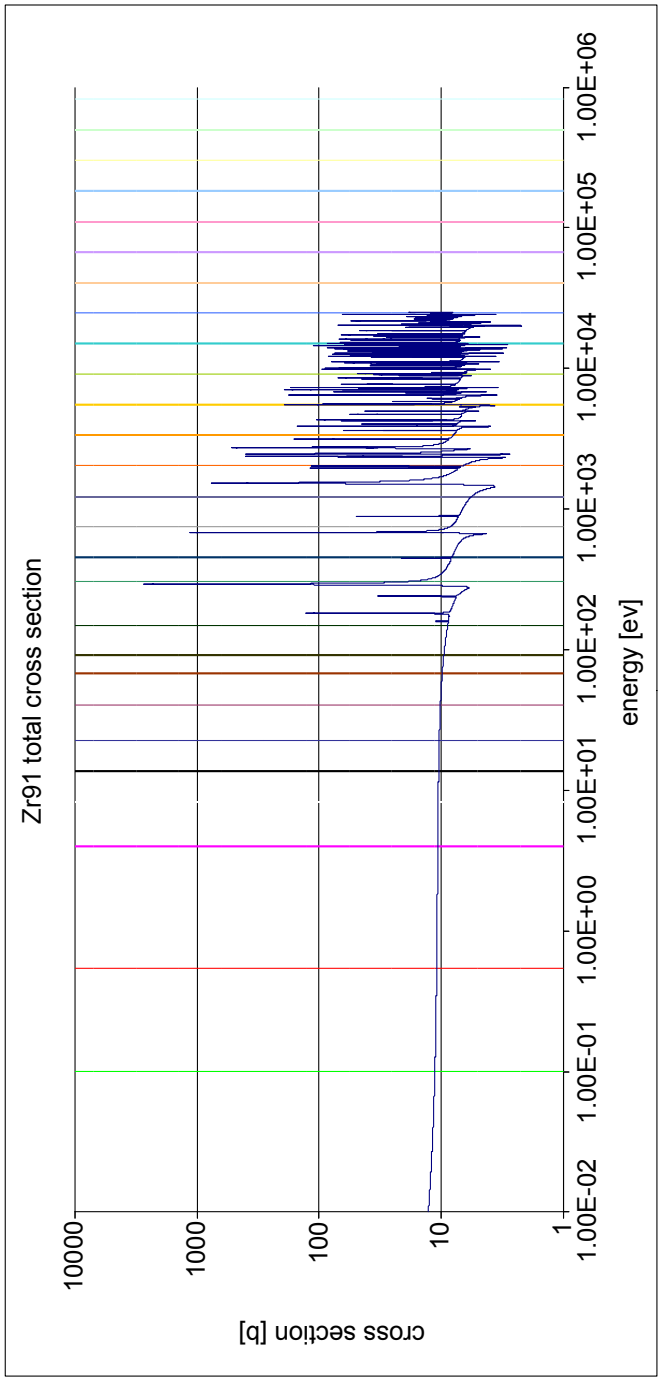

Figure 18: The total cross section of Zr91 from JANIS with JEFF-3.1 data with the standard 33 energy group discretisation by ERANOS pictured by multicolor vertical lines

Table 6: Calculation in 299 energy groups on the simplified finite and infinite cylindrical models. Discrepancy in reactivity between ERANOS and TRIPOLI is reported.

cylinders	$\Delta\rho$ [pcm]
infinite	-42
finite	-198

Table 7: Supplementary energy groups introduced for the treatment in 39 groups. The corresponding group number in 1968 groups and the respective upper energy boundary are listed.

Supplementary energy boundaries	
group number	energy [eV]
1060	3.03E+003
1078	2.61E+003
1097	2.20E+003
1126	1.75E+003
1277	4.99E+002
1311	3.76E+002
1357	2.55E+002
1381	2.08E+002
1407	1.68E+002

As seen by the results, calculations in 39 groups provide an amelioration of about 120 pcm for the infinite and 200 pcm for the finite geometries as can be seen in Table 8. For the infinite cell, the remaining discrepancies of about 100 pcm can be considered satisfactory as the standard deviation for present TRIPOLI calculation ranges typically in the order of 40 to 50 pcm. However, the discrepancies for the finite cells indicate that beyond the energetic correction, further analysis is needed to understand the difference between the probabilistic and deterministic code. A possible element of explanation could be to take into account spatial considerations which can be amplified by the small core size. Some indications are given in the following section 6.2.

Table 8: Discrepancies ERANOS-TRIPOLI in reactivity on cylindrical models with the 39 energy group treatment in ERANOS

Model	$\Delta\rho$ [pcm]
infinite cylinders	
shielding	-27
reflector	-67
refl+shielding	-113
finite cylinders	
shielding	-38
reflector	-305
shielding+reflector	-349

6.2 Spatial Refinements

6.2.1 Fine Macrocell

In contrast to adjustments on the energetic level, spatial adjustments aim to more exactly model the neutron flux within the reactor. A possible approach is the use of macrocells in ECCO [9]. Contrary to the normally used approach where the structure media's cross section gets calculated using the flux of the fissile cell, macrocells permit a more realistic treatment of the flux throughout the structural material. Technically, macrocells do not differ from ordinary cells with no axial buckling as the reactor in whole is represented. They get defined and calculated like ordinary cells in ECCO. However, the last step in the ECCO calculation, the homogenisation (see Chapter 3.2), is not performed. At the transition from ECCO to ERANOS core calculation, the macroscopic selfshielded cross section for each region can be obtained, allowing therefore for the present problem to retrieve cross sections for the reflector. If not mentioned otherwise, the models used in this section are the finite and infinite shielding-reflector-fuel geometries. First, the flux in the reflector was adjusted using macrocell. This implies that a one-dimensional cell was defined containing fuel, reflector and shielding media of the respective radius in a simplified RZ model. As ECCO assumes no flux gradient over one region, the macrocell was divided into parts of about 5 cm width. For the axial considerations, a macrocell was constructed simulating the whole height of a fuel S/A, divided into parts of about 5 cm width. Aliberti et

al. [16] suggest to split the fuel and the reflector part into two regions respectively, a small contact region and a large normal region. For the first test undertaken on the ALLEGRO materials however, all reflector regions of 5 cm got translated from the ECCO cross section calculation into the core calculation in order to get the most exact picture possible whereas the usual cross sections for the fuel and shielding parts were used.
Studies on the infinite and infinite cylinder model containing fuel, shielding and reflector material show very good agreement with the corresponding TRIPOLI values (see Table 9, it compares to table 4). Clearly, the recalculation of the reflector via a macrocell treatment and thus a more realistic flux present an important improvement in the modelling for ALLEGO.

Table 9: Discrepancy in reactivity for ERANOS-TRIPOLI calculated for the radial macrocell on the infinite cylindrical model and for the axial macrocell on the finite cylindrical model. The fuel and shielding parts have normal treatment whereas the reflector area contains regions of 5 cm width ensuing from macrocell calculation.

macrocell	$\Delta\rho$ [pcm]
radial	-52
axial	-210

6.2.2 Axial Buckling Value

In the ECCO cell calculation, the axial buckling value for structural materials has to be defined by the user. The following empiric formula is recommanded [10], where H refers to the characterisitc length or width of the region [18]

$$B^2 = \frac{5}{8}(\frac{\pi}{H})^2 \tag{1}$$

The initial value chosen for H in the case of ALLEGRO was 15 cm for all the structural materials which corresponds to the flat-to-flat S/A distance. By varying this parameter for the structural materials involved over a range for H going from 1 cm to 1000 cm (approaching $B^2 = 0$), namely the reflector, shielding and absorber media, the only medium significantly responding to alteration was the reflector as can be seen from Table 10. All the calculations were carried out with 33 energy group in order to correctly identify

the impacts. The reflector's buckling was then set to an extrapolated radius (height) for the radial (axial) reflector of 40 cm+23 cm=63 cm referring to the simplified finite RZ-model's reflector ring. The buckling for the other structural material got also adjusted correspondingly. Table 11 reports the

Table 10: Variation of the characteristic length for different structural materials, impact on the ERANOS-TRIPOLI discrepancy. Calculations carried out on full RZ model

	$\Delta\rho$ [pcm]
Reflector	
H_{refl}=1	-3149
H_{refl}=1000	-234
Absorber	
H_{abs}=1	-259
H_{abs}=1000	-225
Shielding	
H_{shield}=1	-246
H_{shield}=1000	-244

first test done on the cylindrical models. They show good agreement with the TRIPOLI values. Furthermore, a test done on the homogeneous Hex-Z model gives matching results (see Table 12), when we take into account that the TRIPOLI's standard deviation is for the current calculation about 40 to 50 pcm, hence the discrepancy mostly remains in the range of 3σ. These results are consistent with the ones from macrocell treatment. Adjustment of the buckling value in the ECCO calculation thus represents an adequate way of better modelling the spatial flux. As it is much less time consuming than actual macrocell treatment, it is recommanded to use the possibility of buckling value adjustment rather than macrocell treatment for the same quality of results. However, further verifications to validate this simplified approach should be realised, such as calculation of radial traverses for instance.

6.2.3 Coarse Macrocell

Further studies on the macrocell were undertaken. Especially the application of macrocells to the concrete Hex-Z ALLEGRO model would be interesting as well as the possibility to decrease computing time. Core calculations

Table 11: Discrepancy ERANOS-TRIPOLI on the three RZ models with adjusted axial buckling values

Model	$\Delta\rho$ [pcm]
infinite cylinder fuel+refl +shielding	-32
finite cylinder fuel+refl +shielding	-190
RZ complete	-244

Table 12: Discrepancy ERANOS-TRIPOLI on the homogeneous Hex-Z model using adjusted axial buckling values

Configuration	$\Delta\rho$ [pcm]
Hex-Z all control S/A s out	-93
Hex-Z CSD in	160
Hex-Z CSD+DSD in	286

described in section 6.2.1 use basically a very detailed modelling of the reflector section taking into account regions of 5 centimeters of width. Yet, the good agreement with TRIPOLI values persists if one reduces this detailed description and only uses two reflecting regions in the core calculation: a 5 cm reflector region in contact with the fuel and second one for the rest of the reflector. The cross sections of the first one were always taken from the original region in the macrocell calculation whereas the cross section of the latter were varied: It was either the cross section of a region in the middle part of the reflector or of the outmost region or even the reflector cross sections calculated without macrocells. Results in Tables 13 and 14 for cases of finite and infinite cylinders reveal very good agreement with the TRIPOLI values. It raises the discrepancy determined by the fine macrocell calculation reported in Table 9 only by about 20 pcm. The choice for the cross section of the large region influences the discrepancy by a few pcm. Therefore, the keypoint of the macrocell calculation is to adequatly model the part of the reflector in direct contact with the fuel. A second step which would further simplify macrocell calculation would be to use only two regions in macrocell calculations as suggested by [16]. Results of such calculations with only two regions both in the radial and axial macrocell do show excellent agreement with TRIPOLI. Further, used in the Hex-Z model where the first reflector ring contains a macrocell calculation cross section and the axial reflector also is divided into two parts in agreement with the testing on the simplified

cylindrical models (see Table 15), a certain improvement can be stated as the amplitude of discrepancy with TRIPOLI results is decreased in comparison to results in Chapter 4. However, a macrocell calculation with only two reflecting regions out of which one of them is relatively large (about 35 cm) should preferably not being calculated with ECCO as it requires the flux within a region to be flat.

Table 13: Discrepancy in reactivity ERANOS-TRIPOLI for the finite cylindrical model. Different cases for the second (large) reflector region are reported: Cross sections from macrocell calculations using cross sections from (1) regions in the middle, (2) regions from the outmost part compared to (3) the cross sections from normal ECCO calculations without any macrocell. The first region always uses cross sections from the macrocell calculation

regions used	$\Delta\rho$ [pcm]
middle	-209
outmost	-211
normal	-212

Table 14: Discrepancy in reactivity ERANOS-TRIPOLI for the infinite cylindrical model. Different cases for the second (large) reflector region are reported: Cross sections from macrocell calculations using cross sections from (1) regions in the middle (2) regions from the outmost part compared to (3) the cross sections from normal ECCO calculations without any macrocell. The first region always uses cross sections from the macrocell calculation

Regions used	$\Delta\rho$ [pcm]
middle	-56
outmost	-57
normal	-57

6.3 Combination of Energetic and Spatial Improvements

Tests taking into account the new buckling values in ECCO were run in the 39 group scheme previously proposed in Section 6.1. Results taken from the simplified cylindrical models (see Table 16) show a slight increase of the

Table 15: Discrepancy in reactivity ERANOS-TRIPOLI for the Hex-Z core using simplified macrocell calculations for both radial and axial reflector.

Configuration	$\Delta\rho$ [pcm]
CA out	-216
CA in	233

discrepancy compared to the 33 group scheme with adjusted buckling. Yet, the discrepancies remain in acceptable range.

Table 16: Discrepancy ERANOS-TRIPOLI in reactivity calculated with adjusted axial buckling values on 39 energy groups for cylindrical test models. Comparison of reactivity in ERANOS to initial axial buckling values. The models were either axially finite or infinite fuel cylinders with rings of reflector and shielding.

Simplified RZ-models		
model	$\Delta\rho$ [pcm] ERANOS-TRIPOLI	$\Delta\rho$ [pcm] OldB-NewB
infinite cylinder	-78	-35
finite cylinder	-202	-147

6.4 Control Assembly Worths

ALLEGRO contains ten control S/As, out of which 6 CSD and 4 DSD. Their respective positions can be found schematically in Fig.5. The CAs are basically made of B_4C and SiC absorber pins, containing also small amounts of steel as structural material. The composition of the CSD and DSD S/As is the same in the models looked at. In general, the four CAs located in the inner fuel region were calculated heterogeneously while the 6 outer CAs were calculated homogeneously in consistency with [20]. In the calculations carried out, three cases were distinguished: (1) All CAs out of the core, (2) only the CSD CAs fully inserted in the core and (3) CSD and DSD S/As fully inserted. Concerning the discrepancy, the following behaviour was known from studies on homogeneous Hex-Z cores of ALLEGRO [14] and GFR-2400 [19]: The discrepancy ERANOS-TRIPOLI is negative in the case of all CAs out and gets successively smaller yet positive the more CAs are inserted. This behaviour is broken for the homogeneous Hex-Z ALLEGRO core

when the option of exact transport is used in ERANOS as Table 3 reveals: The discrepancy remains in the same range for different CA configurations. Therefore, the previous changes in discrepancy are probably linked to calculational challenges in ERANOS as mentioned in Chapter 4.2. In addition, a stable discrepancy for different CA configurations can indicate a reliable way of calculation.

Table 17: Discrepancy of the CAs' efficiency $\frac{ERANOS-TRIPOLI}{TRIPOLI}$ in percent for the homogeneous Hex-Z model. Initial values [14] are compared to values obtained from the modified ERANOS model including a 39 energy group treatment and adjusted axial buckling values.

CAs position	Relative discrepancy	
	39 groups and adjusted buckling	33 groups
inner CAs in	5.40%	3.90 %
outer CAs in	-2.50%	-7.0 %

Additionally, a difference in the discrepancy of the CAs' efficieny[3] has been stated for the outer CAs and the inner CAs [20]. The inner CAs' efficiency is over- and the outer CAs' one is underestimated by ERANOS in the range of 2 to 5 %. The changes to a 39 group calculation with adjusted axial buckling values for a Hex-Z calculation of a completely homogeneous core (both CAs and fuel S/As contain homogeneous media) lead to the efficiency discrepancies reported in Table 17. While there is no tremendous change for the inner CAs (5.4 % vs. 3.9 %), the discrepancy for the outer CAs is considerably reduced as the new value of -2.5 % has to be compared to an initial value of -7.0 % [14]. A better treatment of the reflector representing two third of the outer CAs contact material can explain this change.

[3]For these studies distinguishing impacts of outer and inner CA's, all the CAs got calculated homogeneously

7 Conclusions

7.1 Summary

The present work consisted in a investigation of the discrepancy in reactivity between the deterministic code ERANOS-2.1 and the probabilistic code TRIPOLI-4 on the example of the gas cooled fast reactor prototype ALLEGRO in the configuration of ceramic plate type fuel, i.e, the demonstrator core. Both heterogeneous and homogeneous full Hex-Z core models were studied. The option of plate type fuel in ERANOS was validated for ALLEGRO by benchmarking reactivity values against equivalent TRIPOLI models. On the core reactivity, the explicit fuel plate modelling, so-called heterogeneity effect, turned out to be minor. By using simplified models, comparison of TRIPOLI and ERANOS results suggests that the ceramic Zirconium reflector is a relevant element in the modelling and creates most of the discrepancy between the codes. Several ways of adequate Zr modelling in ERANOS were looked at: Refinements on energetic and spatial levels were undergone to understand and take into account the effects of the reflector which provides thermalised neutrons to the core. An improved treatment of the ^{91}Zr resonances by the use of 39 energy groups was developed and successfully tested. The use of macrocells in ERANOS equally lead to a better agreement between the two codes involved. Further, the reflector's axial buckling value used for the ERANOS' cell calculation was shown to be a responsive parameter that can be used as a replacement for time-expensive macrocell calculations. An application of the new modelling method on ALLEGRO states a better treatment of control assemblies in contact with the reflector.
The scientific message of the master thesis work can be summarized as follows:

- *Benchmark of the fuel-plate geometry in ECCO/ERANOS-2.1.* Development of ERANOS and TRIPOLI ALLEGRO demonstrator core models for benchmarking the new fuel-plate treatment geometry in ECCO/ERANOS-2.1. The neutronic deterministic calculations have been verified against the Monte Carlo TRIPOLI4 code. The results have confirmed that the plate-treatment is correctly implemented in ECCO.

- *Heterogeneous vs. homogeneous fuel-plate treatment for ALLEGRO*

demonstrator core. Different core models have been developed in order, additionally to the verification of the fuel plate treatment, to assess the impact of the heterogeneity within the fuel SA (1^{st} heterogeneity level). Based on the results, both in TRIPOLI and ERANOS, the heterogeneity is seen to be small (approximately 40 pcm), while it is important in the large GFR. Different physics considerations have been thought to explain the differences between the two cores. In particular, the ALLEGRO core is a high leakage core (high energy neutrons), has smaller flatto- flat SA and a higher Pu content (approximately 2 times, due to the high leakage). This has an impact in the neutron spectrum (hardness) and mean diffusion length within the fuel plates.

- *ZrC reflector modelling.* The benchmark against TRIPOLI has been realised, in order to understand the reactivity differences, with simplified core models as well. This has allowed to identify that the ZrC reflector is mainly responsible for the reactivity differences in ERANOS. Since the core is small, the impact in the neutron balance of the reflector is particularly important and special care has to be taken to model the ceramic reflector.

- *Derive a computational scheme in ERANOS for ALLEGRO demonstrator-core against TRIPOLI4 calculations.* In ERANOS, the axial buckling B^2 is adjusted in sub-critical media. The present work has studied the impact of different buckling values and comparison was made using the *macrocell* treatment in ECCO, which basically reproduces at the cell level, a representative core zone to evaluate the multi-group self-shielded cross-sections. A refinement of the broad 33 group structure featuring a 39 group structure was proposed and the validation against a 299 group treatment was realised. By adjusting the energy group structure and the buckling value, the advantage of the *macrocell* is reproduced with the advantage of avoiding large CPU time calculations.

7.2 Future Work

Future work may continue in various directions: The benchmark between the two codes could be analyzed in more extension by taking into account additional parameters as the neutron balance or reaction rate tranverses using both codes. This would include studies on reaction rate, spectral indices,

weights of individual control assemblies and power distribution. After completion of these additional tests, heterogeneity of ALLEGRO under operating conditions can be studied.
The heterogeneous TRIPOLI core model and the corresponding ERANOS core model are only equivalent under some restrictions due to approximations in the cell modelling. To separate effects due to the assumptions taken from effects arising from the plate-type modelling in ERANOS and TRIPOLI, an exact counterpart of the ERANOS' one should be established in TRIPOLI. Further, the use of energy groups in TRIPOLI instead of pointwise cross sections is to be explored in more detail. In addition, a comparison GFR-2400 and ALLEGRO in terms of the heterogeneity's impact may be conducted.
The 39 group treatment has to be validated and analysed for other elements present in ALLEGRO in order to find energy boundaries that take into account of all resonances in an optimized way. Further, the impact of a treatment with a higher number of groups, 299 or even 1968 in a Hex-Z core model would be desirable.
Concerning an adequate modelling of the reflector in ECCO/ERANOS, special care must be taken of the control assemblies mainly in contact with the reflector. One could think of macrocell treatment based modelling for the control assemblies. Further, the impact on the ERANOS -TRIPOLI discrepancy by the use of different cross section libraries would lead to a further insight into the problem.

8 Acknowledgement

This master thesis bases on work carried out at the Commissariat à l'Énergie Atomique (CEA), Cadarache, France. I wish to thank all the people involved who made this fruitful collaboration possible. Special thanks to Valérie Brun-Magaud for her help and support during and after my stay.

References

[1] Pradel P (dir), *Les réacteurs à caloporteurs gaz*, ISBN10 : 2-281-11317-5 (2006)

[2] Poette C et al, *GFR Demonstrator ALLEGRO Design Status* Proceedings of ICAPP 09 **9062** (2009)

[3] Both J P et al, *User Manual for version 4.3 of the TRIPOLI Monte Carlo method particle transport computer code* CEA-Report : CEA-R-6044, DTI, CEA/Saclay (2003)

[4] Both J P et al, *TRIPOLI a Three Dimensional Polykinetic Particle Transport Monte Carlo Code* Proceedings of ICAPP (2003)

[5] Ruggieri J M et al, *ERANOS: International Code System for GEN IV Fast Reactor Analysis* Proceedings of ICAPP 06 **6360**(2006)

[6] Rimpaul G et al., *The ERANOS Data and Code System for Fast Reactor Neutronic Analysis* Proceedings of International conference On the New Frontier of Nuclear Technology: Reactor Physics, Safety and High-Performance Computing, PHYSOR (2002)

[7] Palmiotti G et al *BISTRO Optimized Two Dimensional Sn Transport Code*, Topical Meeting on Advances in Reactor (1987)Physics, Mathematics and Computation, Paris (1987)

[8] Palmiotti G et al., *VARIANT: Variational Anisotropic Nodal Transport for Multidimensional Cartesian and Hexagonal Geometry Calculation*, Technical Report, ANL-95/40, Argonne National Laboratory (1995)

[9] Dean C J et al, *Production of Fine Group Data for the Ecco code* ANS Topical Meeting on Reactor Physics PHYSOR (1990)

[10] **ERANOS code online documentation** http://fast. web. psi. ch/intranet/ERANOS/HTML_ERANOS_2.1/ 13.01.2010

[11] Da Cruz DF et al., *Neutronic benchmark on the 2400 MW gas-cooled fast reactor design* ANS Topical Meeting on Reactor Physics PHYSOR (2006)

[12] Bosq J C, Peneliau Y, Rimpault G, Vanier M, *Fine 3D neutronic characterisation of a gas cooled fast reactor based on plate -type subassemblies* (2006)

[13] Girardin G, *Development of the Control Assembly Pattern and Dynamic Analysis of the Generation IV Large Gas-cooled Fast Reactor* PhD thesis **no 4437** Ecole Polytechnique Fédérale de Lausanne (2009)

[14] Brun V *Caractérisation neutronique du coeur ALLEGRO de démonstration à plaques céramiques et de puissance 75MWth* CEA report 09-427, DER/SPRC, CEA/Cadarache (2009)

[15] Bell GI, Glasstone S. *Nuclear Reactor Theory*, ISBN 0-88275-790-3(1970)

[16] Aliberti G, Palmiotti G, Salvatores M, *Methodologies for Treatment of Spectral Effects at Core-Reflector Interfaces in Fast Neutron Systems* ERANOS Users' Workshop (2006)

[17] Varaine F, Peneliau Y, *Calculation of Moderated Subassembly Experiments in PHENIX* ERANOS Users' Workshop (2006)

[18] Rimpault G, Suteau C *Lattice Calculation with ECCO* ERANOS Users' Workshop 2006

[19] Private discussion with V. Brun, (2009)

[20] Brun V, *ALLEGRO-Etude neutronique du coeur démonstrateur à plaques 75 MWth* Revue d'avancement RAGAZ du 19 juin (2009)

9 Appendix A

Table 18: Sensitivity analysis on isotopes for both the infinite cell and the reactor.

Reactor						
ISOTOPE	CAPTURE	ELASTIC	INELASTIC	FISSION	N,XN	SUM
C	-1.11E-007	1.56E-005	-2.89E-007	0.00E+000	0.00E+000	1.52E-005
Si28	1.92E-006	2.46E-006	4.73E-006	0.00E+000	-1.41E-012	9.11E-006
U235	1.97E-007	-3.71E-009	-3.80E-007	9.17E-006	1.99E-008	9.01E-006
U238	4.79E-005	-1.09E-006	-7.22E-005	1.35E-004	3.40E-006	1.13E-004
Pu238	1.11E-006	-8.55E-009	-2.85E-007	2.02E-005	9.71E-009	2.11E-005
Pu239	2.85E-005	-1.44E-007	-6.57E-006	3.89E-004	2.39E-007	4.11E-004
Pu240	1.51E-005	-8.82E-008	-3.91E-006	9.50E-005	8.00E-008	1.06E-004
Pu241	2.80E-006	-2.01E-008	-9.82E-007	7.12E-005	1.51E-007	7.31E-005
Pu242	3.21E-006	-2.41E-008	-1.34E-006	2.24E-005	4.71E-008	2.42E-005
Cell						
C	1.38E-008	-3.52E-005	-3.11E-007	0.00E+000	0.00E+000	-3.55E-005
Si28	3.57E-006	9.78E-007	5.01E-006	0.00E+000	-1.12E-012	9.56E-006
U235	-1.56E-006	-8.97E-009	-4.47E-007	6.89E-006	1.51E-008	4.89E-006
U238	-3.85E-005	-1.61E-006	-8.08E-005	4.99E-005	2.58E-006	-6.85E-005
Pu238	-1.94E-006	-1.80E-008	-3.27E-007	1.12E-005	7.48E-009	8.88E-006
Pu239	-2.25E-005	-3.10E-007	-7.72E-006	2.71E-004	1.73E-007	2.41E-004
Pu240	-1.17E-005	-1.68E-007	-4.49E-006	4.24E-005	6.11E-008	2.61E-005
Pu241	-5.98E-006	-4.13E-008	-1.11E-006	5.47E-005	1.14E-007	4.77E-005
Pu242	-5.40E-006	-4.98E-008	-1.54E-006	9.82E-006	3.35E-008	2.87E-006